# Longitudinal relaxation of a nitrogen-vacancy center in a spin bath by generalized cluster-correlation expansion method

Zhi-Sheng Yang [a], Yan-Xiang Wang [a], Ming-Jie Tao [a], Wen Yang [b], Mei Zhang [a], Qing Ai [a,*], Fu-Guo Deng [a,c]

[a] *Department of Physics, Applied Optics Beijing Area Major Laboratory, Beijing Normal University, Beijing 100875, China*
[b] *Beijing Computational Science Research Center, Beijing 100094, China*
[c] *NAAM-Research Group, Department of Mathematics, Faculty of Science, King Abdulaziz University, Jeddah 21589, Saudi Arabia*

A R T I C L E   I N F O

A B S T R A C T

We theoretically study the longitudinal relaxation of a nitrogen-vacancy (NV) center surrounded by a $^{13}$C nuclear spin bath in diamond. By incorporating electron spin in the cluster, we generalize the cluster-correlation expansion (CCE) to theoretically simulate the population dynamics of the electron spin of the NV center. By means of the generalized CCE, we numerically demonstrate the decay process of the electronic state induced by cross relaxation at ambient temperature. It is shown that the CCE method is not only capable of describing pure-dephasing effects in the large-detuning regime, but it can also simulate the quantum dynamics of populations in the nearly-resonant regime.
© 2019 Elsevier Inc. All rights reserved.

## 1. Introduction

Nitrogen-vacancy (NV) center is a pair of point defects in the diamond lattices [1,2]. It is comprised of a substitutional nitrogen atom and a vacancy at the adjacent lattice. Because of possessing $S = 1$ electron spin, the ground-state manifold of the negatively-charged NV center is triplet states and it can be optically initialized and measured.

---

* Corresponding author.
  *E-mail address:* aiqing@bnu.edu.cn (Q. Ai).

For a sample of high purity, the NV center possesses a long coherence time and can be further prolonged, to approach one second, by dynamical decoupling [3,4]. It can be coherently controlled by microwave fields and is highly sensitive to external electric and magnetic fields. These superior characteristics make the NV center a promising candidate for quantum information processing [5–10], imaging beyond the diffraction limit [11], as well as quantum sensing of electric and magnetic fields [12–14], temperature [15], stress [16], biological structures [17] and chemical reactions [18]. In addition, the NV centers can be coupled with other kinds of quantum systems, e.g. carbon nanotubes [19], flux qubits [20], and piezomagnetic superlattices [21], which can be structured as promising hybrid quantum devices [22,23]. Such appealing applications require full knowledge of its decoherence behavior, including both transverse and longitudinal relaxation [24–26], over a broad range of physical parameters, such as temperature, magnetic field, type and concentration of impurities. Among quantum many-body theories for many-spin bath dynamics [27–30], e.g. the density matrix cluster expansion [31–33], the pair correlation approximation [34–36], and the linked-cluster expansion [37], the cluster-correlation expansion (CCE) [38–40] developed by one of the authors, WY, has been successfully applied to describe the pure-dephasing process of a central spin coupling to a many-spin bath in the largely-detuned regime [41]. By the CCE approach, the anomalous decoherence effect of NV center in a quantum spin bath has been theoretically predicted [42] and experimentally verified [43]. Interestingly, the decoherence of NV center, which was previously considered as an obstacle to realize quantum computation [44,45], has been explored to detect a remote nuclear spin dimer [46] and proposed for navigation by using the weak geomagnetic field [40]. Similarly, it was recently shown that a quantum system, e.g. the NV center, can be explored to obtain the information of a boson bath [47].

Meanwhile, the experimental investigation on the longitudinal relaxation of NV center has been delicately performed for a broad range of temperature, magnetic field, concentration of impurities, ever since 1991 [48–51]. The physical mechanism of longitudinal relaxation above 100 K is attributed to Orbach and Raman phonon process [48,49]. When the temperature reaches as low as a few tens of kelvins, $T_1$ clearly demonstrates dependence on the concentration of magnetic impurities [49]. In addition, when varying the magnetic field, $T_1$ abruptly drops around some energy-level anti-crossing points [49]. These observations motivate us to develop a theory to describe the longitudinal relaxation of NV center in a quantum many-spin bath. In this paper, by including the electron spin in the cluster expansion, we generalize the CCE to simulate the quantum dynamics of NV center exchanging population with a nuclear spin bath in the nearly-resonant regime.
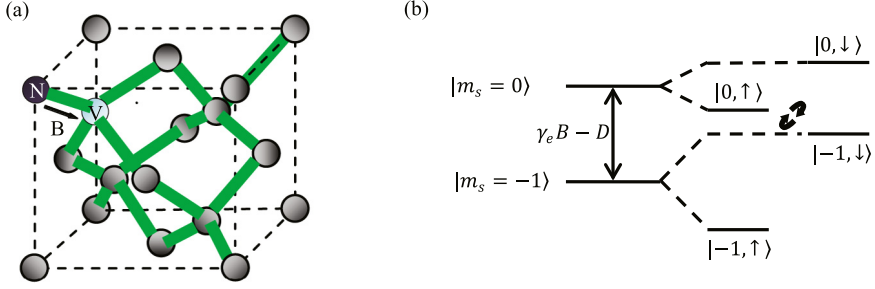
When a static magnetic field is applied to make the NV center close to the level anticrossing point, the hyperfine interaction of the NV center with the $^{13}C$ nuclear spins induces the NV electron spin relaxation. The numerical simulation with the CCE approach yields a convergent result and thus is capable of fully describing the NV electron spin relaxation induced by the $^{13}C$ spin bath.

This paper is organized as follows: In Section 2, we present our system model. In Section 3, we show the CCE approach after generalization. In Section 4, we simulate the longitudinal relaxation of NV center surrounded by $^{13}C$ nuclear bath with the generalized CCE. A detailed discussion and a summary are enclosed in Section 5.

## 2. Model

As shown in Fig. 1, a negatively-charged NV center is coupled to the $^{13}C$ nuclear spins randomly located at the diamond lattices, with the natural abundance of $^{13}C$ being 1.1% [52]. Here, since we focus on the longitudinal relaxation induced by $^{13}C$ nuclear spins far away from the NV center, in our numerical simulation we use the randomly-generated bath in which there is no $^{13}C$ nuclear spin in the vicinity of NV center [52]. The NV center consists of a substitutional nitrogen atom adjacent to a vacancy. The ground state of NV center is a triplet state with $m_s = 0$ and $m_s = \pm 1$ denoted by $|0\rangle$ and $|\pm 1\rangle$ respectively. When there is no magnetic field applied to the NV center, $|\pm 1\rangle$ are degenerate and they are separated from $|0\rangle$ by zero-field splitting $D = 2.87$ GHz [1,2]. In an external magnetic field $B_z$ along the NV axis, the degeneracy between $m_s = \pm 1$ levels are lifted and thus the full Hamiltonian of the total system describing the NV center and spin bath is

$$H = H_{NV} + H_{bath} + H_{int}, \tag{1}$$

**Fig. 1.** (Color online) Schematic illustration of an NV center surrounded by a spin bath. (a) An NV center in the crystal structure of a diamond, where a static magnetic field is applied along the principal axis of NV center. (b) The hyperfine structure of an NV center and one $^{13}C$ nuclear spin in the bath.

where the Hamiltonian of the NV center has the form

$$H_{NV} = DS_z^2 - \gamma_e B_z S_z \tag{2}$$

with $\gamma_e = -1.76 \times 10^{11}$ rad s$^{-1}$ T$^{-1}$ being the electronic gyromagnetic ratio [52] and $S_z = |1\rangle\langle 1| - |-1\rangle\langle -1|$.

The Hamiltonian of the bath reads

$$H_{bath} = \sum_{i<j} D_{ij} \left[ \mathbf{I}_i \cdot \mathbf{I}_j - \frac{3\left(\mathbf{I}_i \cdot \mathbf{r}_{ij}\right)\left(\mathbf{r}_{ij} \cdot \mathbf{I}_j\right)}{r_{ij}^2} \right]$$
$$- \gamma_c B_z \sum_i I_i^z, \tag{3}$$

where the gyromagnetic ratio of $^{13}C$ nuclear spin is [52] $\gamma_c = 6.73 \times 10^7$ rad s$^{-1}$ T$^{-1}$,

$$D_{ij} = \frac{\mu_0 \gamma_c^2}{4\pi r_{ij}^3} \left( 1 - \frac{3\mathbf{r}_{ij}\mathbf{r}_{ij}}{r_{ij}^2} \right) \tag{4}$$

is the magnetic dipole–dipole interaction between the $i$th and $j$th $^{13}C$ nuclear spins with $\mathbf{r}_{ij}$ being the displacement vector from $i$th to $j$th spins and $\mu_0$ being the vacuum permeability.

The electron spin and nuclear spins are coupled by hyperfine interaction. Because we are interested in a large number of $^{13}C$ nuclear spins far away from the NV center, the hyperfine interaction is mainly described by magnetic dipole–dipole interaction and thus the interaction Hamiltonian is

$$H_{int} = \mathbf{S} \cdot \sum_i A_i \cdot \mathbf{I}_i, \tag{5}$$

where

$$A_i = \frac{\mu_0 \gamma_c \gamma_e}{4\pi r_i^3} \left( 1 - \frac{3\mathbf{r}_i \mathbf{r}_i}{r_i^2} \right) \tag{6}$$

is the hyperfine coupling tensor, $\mathbf{r}_i$ is the position vector of $i$th nuclear spin, and the position of NV center is chosen as the origin.

## 3. Generalized cluster-correlation expansion

In this section, by taking electron spin into consideration in the cluster, we generalize the CCE method [38,39] to describe the electron spin relaxation in a spin bath. We choose the CCE method instead of other quantum many-body theories mentioned in Section 1, because it can embrace some
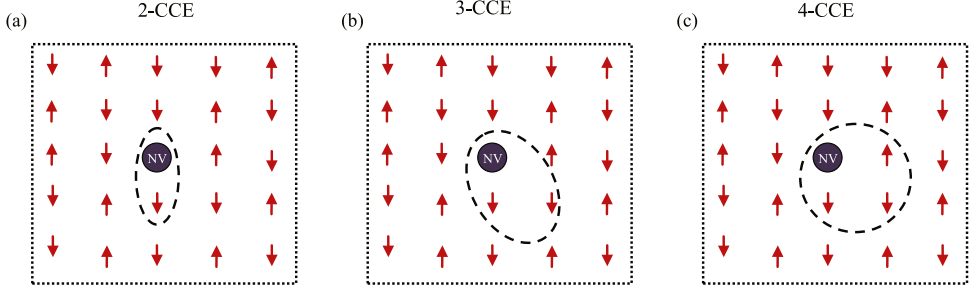
**Fig. 2.** (Color online) Schematic of generalized CCE. The bath of $^{13}$C nuclear spins and the NV center forms an open quantum system. The $^{13}$C atoms with 1/2 nuclear spin denoted by the small red arrows are randomly located on the diamond lattice. (a) 2-CCE: A cluster containing one bath spin and the NV center. (b) 3-CCE: A cluster containing two bath spins and the NV center. (c) 4-CCE: A cluster containing three bath spins and the NV center. The spins outside the cluster are assumed to be frozen when calculating the cluster contribution.

possible important clusters, which may have nonnegligible influence on the longitudinal relaxation within a spatial distance. Traditional CCE method has been successfully applied to calculating the pure dephasing of an NV center in the large-detuning regime. However, the central spin flip must be considered when the energy relaxation of the NV center is involved in the nearly-resonant regime.

Assuming that the bath consists of spin $i$ only, cf. Fig. 2(a), the probability $P(t)$ of NV center in the state $|0\rangle$ is explicitly calculated as

$$\tilde{P}_{\{i\}} = P_{\{i\}} \equiv \frac{\text{Tr}\left(\rho(0)e^{iH_{\{i\}}t}|0\rangle\langle 0|e^{-iH_{\{i\}}t}\right)}{\text{Tr}\left(\rho(0)e^{iH_{\text{NV}}t}|0\rangle\langle 0|e^{-iH_{\text{NV}}t}\right)}, \tag{7}$$

where $\rho(0)$ is the initial state of the total system including the NV center and nuclear spin bath,

$$H_{\{i\}} = H_{\text{NV}} - \gamma_c B_z I_i^z + \mathbf{S} \cdot A_i \cdot \mathbf{I}_i \tag{8}$$

is obtained from Eq. (1) by dropping all terms other than spin $i$.

Assuming that the bath consists of spin $i$ and spin $j$, cf. Fig. 2(b), $P(t)$ reads

$$P_{\{i,j\}} \equiv \frac{\text{Tr}\left(\rho(0)e^{iH_{\{i,j\}}t}|0\rangle\langle 0|e^{-iH_{\{i,j\}}t}\right)}{\text{Tr}\left(\rho(0)e^{iH_{\text{NV}}t}|0\rangle\langle 0|e^{-iH_{\text{NV}}t}\right)}, \tag{9}$$

where

$$\begin{aligned}
H_{\{i,j\}} &= H_{\text{NV}} - \gamma_c B_z \sum_{\alpha=i,j} I_\alpha^z + \mathbf{S} \cdot \sum_{\alpha=i,j} A_\alpha \cdot \mathbf{I}_\alpha \\
&\quad + D_{ij}\left[\mathbf{I}_i \cdot \mathbf{I}_j - \frac{3\left(\mathbf{I}_i \cdot \mathbf{r}_{ij}\right)\left(\mathbf{r}_{ij} \cdot \mathbf{I}_j\right)}{r_{ij}^2}\right]
\end{aligned} \tag{10}$$

is calculated from Eq. (1) by dropping all terms other than spin $i$ and spin $j$, and the spin-pair correlation is

$$\tilde{P}_{\{i,j\}} \equiv \frac{P_{\{i,j\}}}{\tilde{P}_{\{i\}}\tilde{P}_{\{j\}}}. \tag{11}$$

Assuming that the bath consists of three spins $i$ and $j$ and $k$, cf. Fig. 2(c), $P(t)$ in this case becomes

$$P_{\{i,j,k\}} \equiv \frac{\text{Tr}\left(\rho(0)e^{iH_{\{i,j,k\}}t}|0\rangle\langle 0|e^{-iH_{\{i,j,k\}}t}\right)}{\text{Tr}\left(\rho(0)e^{iH_{\text{NV}}t}|0\rangle\langle 0|e^{-iH_{\text{NV}}t}\right)}, \tag{12}$$

where

$$
H_{\{i,j,k\}} = H_{NV} - \gamma_c B_z \sum_{\alpha=i,j,k} I_\alpha^z + \mathbf{S} \cdot \sum_{\alpha=i,j,k} A_\alpha \cdot \mathbf{I}_\alpha
$$

$$
+ \sum_{\alpha=i,j,k} \sum_{\beta>\alpha} D_{\alpha\beta} \left[ \mathbf{I}_\alpha \cdot \mathbf{I}_\beta - \frac{3 \left( \mathbf{I}_\alpha \cdot \mathbf{r}_{\alpha\beta} \right) \left( \mathbf{r}_{\alpha\beta} \cdot \mathbf{I}_\beta \right)}{r_{\alpha\beta}^2} \right] \tag{13}
$$

is calculated from Eq. (1) by dropping all terms other than the three spins $i$ and $j$ and $k$, and the three-spin correlation is

$$
\tilde{P}_{\{i,j,k\}} \equiv \frac{P_{\{i,j,k\}}}{\tilde{P}_{\{i\}} \tilde{P}_{\{j\}} \tilde{P}_{\{k\}} \tilde{P}_{\{i,j\}} \tilde{P}_{\{j,k\}} \tilde{P}_{\{k,i\}}}. \tag{14}
$$

For the bath with arbitrary number of spins, $P(t)$ is generalized as

$$
P_{\mathfrak{c}} \equiv \frac{\text{Tr} \left( \rho(0) e^{iH_{\mathfrak{c}} t} |0\rangle\langle 0| e^{-iH_{\mathfrak{c}} t} \right)}{\text{Tr} \left( \rho(0) e^{iH_{NV} t} |0\rangle\langle 0| e^{-iH_{NV} t} \right)}, \tag{15}
$$

where $H_{\mathfrak{c}}$ is obtained from Eq. (1) by dropping all terms other than spins in the cluster $\mathfrak{c}$, and the spin-cluster correlation is

$$
\tilde{P}_{\mathfrak{c}} \equiv \frac{P_{\mathfrak{c}}}{\prod_{\mathfrak{c}'\subset\mathfrak{c}} \tilde{P}_{\mathfrak{c}'}}. \tag{16}
$$

Furthermore, in Eqs. (7), (9), (12), (15), all of the denominators are equal to unity because the system is initially prepared at $|0\rangle$, which is also the eigenstate of $H_{NV}$.

Generally speaking, it is impossible to exactly calculate $P(t)$ for a large number of spins as the dimension of Hilbert space scales exponentially with the number of spins. The $M$-CCE method approximates $P(t)$ as

$$
P^{(M)} = \prod_{|\mathfrak{c}|\leq M} \tilde{P}_{\mathfrak{c}}, \tag{17}
$$

where $|\mathfrak{c}|$ is the number of spins in the cluster $\mathfrak{c}$. For example, the first-order truncation of $P(t)$ yields

$$
P^{(1)} = \prod_i \tilde{P}_{\{i\}}. \tag{18}
$$

And the second-order truncation of $P(t)$ reads

$$
P^{(2)} = \prod_i \tilde{P}_{\{i\}} \prod_{i,j} \tilde{P}_{\{i,j\}}. \tag{19}
$$

## 4. Decay of NV center induced by nuclear spin bath

In this section, we discuss the longitudinal relaxation of electron spin of NV center induced by coupling to the nuclear spin bath. When the energy gap between $|0\rangle$ and $|-1\rangle$ approaches the energy gap of $^{13}$C nuclear spins, e.g. by tuning the magnetic field, the electron spin exchanges polarization with nuclear spins, cf. Fig. 1(c), and the longitudinal relaxation of electronic spin occurs. For simplicity, we consider the situation of low temperature and a single NV in the diamond, so that the decay of electron spin is mainly due to hyperfine interaction with nuclear spins, and the effect of diamond lattice phonons on the relaxation is beyond the scope of the present investigation.

The state of electronic spin can be optically initialized into $|0\rangle$, corresponding to the density matrix

$$
\rho_{NV} = |0\rangle\langle 0|. \tag{20}
$$

In principle, the $^{13}$C nuclear spin bath should be in the thermal equilibrium state since the typical experimental temperature is much higher than the nuclear spin Zeeman splitting, even in a strong
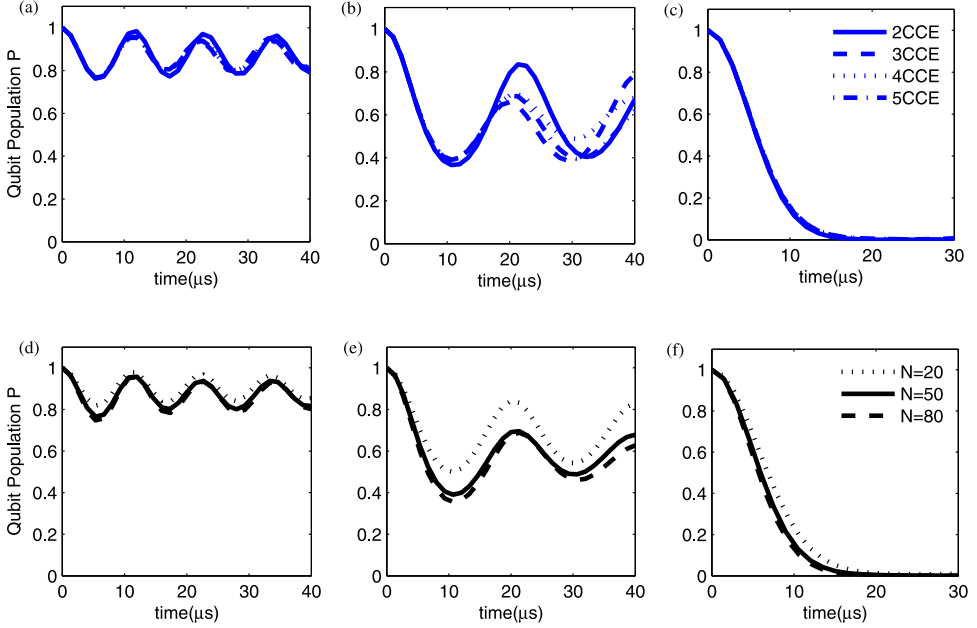
**Fig. 3.** (Color online) The longitudinal relaxation process of the NV center under different magnetic fields. Survival probability of initial state of electron spin by different orders of CCE with $N = 50$ and (a) $B_z = 1025.01$ G, (b) $B_z = 1024.99$ G, (c) $B_z = 1024.97$ G. Survival probability with different bath sizes and (d) $B_z = 1025.01$ G, (e) $B_z = 1024.99$ G, (f) $B_z = 1024.97$ G.

magnetic field, e.g. several T. Therefore, without loss of generality, we take the density matrix of the $^{13}$C bath as

$$\rho_B = \frac{1}{2^N} \prod_{i=1}^{\otimes N} (|\uparrow\rangle_i\langle\uparrow| + |\downarrow\rangle_i\langle\downarrow|), \tag{21}$$

where $|\uparrow\rangle_i$ $(|\downarrow\rangle_i)$ is the spin-up (spin-down) state of the $i$th $^{13}$C nuclear spin, with the quantization axis along the N-V symmetry axis. As a result, the density matrix of total system at the initial time is

$$\rho(0) = \rho_{NV} \otimes \rho_B. \tag{22}$$

The evolution of the coupled system is given by

$$\rho(t) = e^{-iHt} \rho(0) e^{iHt}. \tag{23}$$

By partially tracing over the degrees of freedom of the bath, we could obtain the survival probability of the initial state $|0\rangle$ of the NV electron spin as

$$P(t) = \text{Tr}_B\langle 0|e^{-iHt} \rho(0) e^{iHt}|0\rangle. \tag{24}$$

For a small spin bath, we can exactly calculate the longitudinal relaxation of electron spin via Eq. (24). However, with increasing size of the nuclear spin bath, this approach quickly becomes unfeasible, because the dimension of the Hilbert space grows exponentially with the number of nuclei [53,54]. In this case, an approximate many-body theory with high performance has to be considered. In previous works, the CCE theory has been successfully applied to describe the pure dephasing of a central spin in a spin bath [38,39,42,46]. Here, we generalize the CCE theory to deal with the longitudinal relaxation of the electron spin in a spin bath. In Fig. 3(a), we numerically simulate the survival probability of the initial state of electron spin surrounded by $N = 50$ nuclear
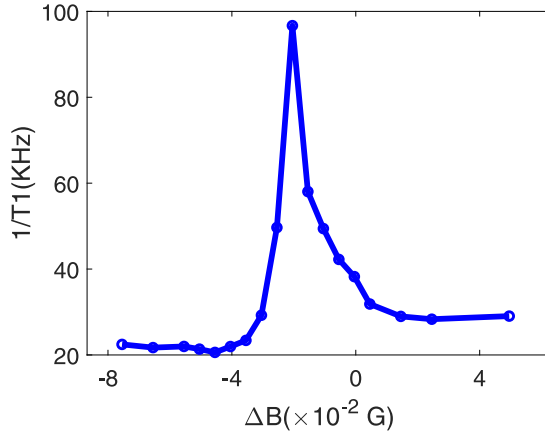
**Fig. 4.** (Color online) The longitudinal electron-spin relaxation time ($T_1$) of the NV center under different magnetic fields $\Delta B = B - 1025$ G at 4-CCE.

spins under the magnetic field intensity $B_z = 1025.01454$ G along the NV axis. When the order of CCE method is increased, the results quickly converge, e.g., the differences between the results obtained from 4-CCE and 5-CCE are indistinguishable. This suggests that 4-CCE already offers a reliable solution to the quantum dynamics of central spin under the influence of a many-spin bath, and thus we choose the 4-CCE to illustrate Fig. 4. Fig. 3(a) shows the population of electron spin experiences a damped oscillation with a small amplitude because there is still a large energy gap between the electron spin and nuclear spin as compared to their hyperfine interaction. When we reduce the energy gap of electron spin by tuning the magnetic field, cf. Fig. 3(b), both the amplitude and period of damped oscillation become larger as the electron and nuclear spins are getting close to resonance. If we further tune the electronic level to the nearly-resonant case, as shown in Fig. 3(c), the population of electronic initial state decays to zero around 10 µs without collapse and revival. When the electron spin resonantly interacts with a nuclear spin, its population will demonstrate Rabi oscillation with full amplitude and frequency $A_i$. Since all nuclear spins interact with the electron spin with different hyperfine interactions, the electronic population will irreversibly decay and no revival will occur. Furthermore, we explore the effect of the bath's size on the relaxation. In Fig. 3(d), the population dynamics of the electron spin is investigated for $^{13}$C baths of different sizes with a large energy gap. When the size of the bath is increased, the difference before and after the change becomes more and more negligible. As further enlarging the size will not significantly decrease the difference but result in much more computation time, the 4-CCE theory with a bath of $N = 50$ nuclear spins already yields a reliable result, as confirmed in Fig. 3(e) and (f).

Furthermore, we numerically fit the relaxation process by an exponential decay, and show the longitudinal electron-spin relaxation time ($T_1$) under different magnetic fields at 4CCE and $N = 50$ in Fig. 4. It shows that $1/T_1$ varies sensitively in response to the change of the magnetic field. Especially, when the magnetic field is tuned to the resonance point, i.e., 1024.975 G, $1/T_1$ has been increased by nearly one order of magnitude. This result is reasonable since around the resonance, many different nuclear spins can exchange spin with the electron with different frequencies and thus result in enhanced decoherence. It is consistent with experimental investigation shown in Ref. [49], where electronic decoherence around the resonance was enhanced by coupling to nitrogen nuclear-spin bath. In our work, at the resonance $T_1^{-1}$ is 97.1 kHz for a bath with $^{13}$C concentration 1.1%, while in Ref. [49] $T_1^{-1} = 0.800$ kHz at 20 K and $B = 514$ G. The ratio of $^{13}$C's to $^{14}$N's nuclear spin magnetic moment is 0.702/0.404 [55,56]. For a bath with $^{14}$N concentration 40∼60 ppm, the estimated $T_1^{-1} = 0.117 \sim 0.175$ kHz, which is qualitatively in agreement with the experimental observation.

## 5. Discussion and summary

In this paper, by embodying the electron spin in the cluster, we generalize the CCE approach to deal with the longitudinal relaxation of a central electron spin due to its couplings to a nuclear spin bath in diamond. In the largely-detuned case, because the electron spin cannot effectively exchange energy with the nuclear spins, the couplings to the nuclear spin bath manifest as the pure-dephasing phenomenon of the NV center [52]. Since the pure-dephasing effect is sensitive to the local magnetic field at the NV center, it can be fully utilized to detect magnetic source with internal structure [46].

When getting close to the degenerate point, we show diverse decay phenomena of initial state's population by tuning the magnetic field. When the energy gap of electronic levels is small but not too small, only a few nuclear spins can exchange population with the electron spin. It results in a damped oscillation with a very small decay rate. If we further reduce the energy gap, a more remarkable damped oscillation can be observed as more nuclear spins can be probed by the electron spin. When the electron spin is finally tuned to be in resonance with all nuclear spins, the population of initial state will monotonically decay and no revival will take place.

We consider the feasibility with the current accessible parameters in the experiments. The state of NV center $|0\rangle$ can be initialized by applying 532 nm laser [1]. In order to bring the electronic spin close to the degenerate point, a magnetic field with strength $B_z \approx 1025$ G should be applied to NV center, which is available at current laboratory conditions [57]. After the optical pumping, the NV center will be left to evolve under the influence of nuclear spin bath for an interval and then readout by detecting the fluorescence after spin-dependent optical excitation [58].

In this paper, because of the generalization, the CCE approach is capable of describing the quantum evolution of the whole density matrix of the system including both the off-diagonal and diagonal terms. Recently, quantum coherent energy transfer has attracted broad interest from different disciplines.

## Declaration of competing interest

The authors declare that they have no known competing financial interests or personal relationships that could have appeared to influence the work reported in this paper.

## Acknowledgments

## References

[1] M.W. Doherty, N.B. Manson, P. Delaney, F. Jelezko, J. Wrachtrup, L.C.L. Hollenberg, Phys. Rep. 528 (2013) 1.
[2] V.V. Dobrovitski, G.D. Fuchs, A.L. Falk, C. Santori, D.D. Awschalom, Annu. Rev. Condens. Matter Phys. 4 (2013) 23.
[3] G. de Lange, Z.H. Wang, D. Ristè, V.V. Dobrovitski, R. Hanson, Science 330 (2010) 60.
[4] N. Bar-Gill, L.M. Pham, A. Jarmola, D. Budker, R.L. Walsworth, Nature Commun. 4 (2013) 1743.
[5] L. Childress, J.M. Taylor, A.S. Sørensen, M.D. Lukin, Phys. Rev. Lett. 96 (2006) 070504.
[6] M.V.G. Dutt, L. Childress, L. Jiang, E. Togan, J. Maze, F. Jelezko, A.S. Zibrov, P.R. Hemmer, M.D. Lukin, Science 316 (2007) 1312.
[7] A.M. Zagoskin, J.R. Johansson, S. Ashhab, F. Nori, Phys. Rev. B 76 (2007) 014122.
[8] M.-J. Tao, M. Hua, Q. Ai, F.-G. Deng, Phys. Rev. A 91 (2015) 062325.
[9] X.K. Song, H. Zhang, Q. Ai, J. Qiu, F.-G. Deng, New J. Phys. 18 (2016) 023001.
[10] Y.-Y. Wang, J. Qiu, Y.-Q. Chu, M. Zhang, J.-M. Cai, Q. Ai, F.-G. Deng, Phys. Rev. A 97 (2018) 042313.
[11] Q. Ai, P.-B. Li, W. Qin, C.P. Sun, F. Nori, NV-Metamaterial: Tunable quantum hyperbolic metamaterial using nitrogen-vacancy centers in diamond, 2018, arXiv:1802.01280.
[12] F. Dolde, H. Fedder, M.W. Doherty, T. Nobauer, F. Rempp, G. Balasubramanian, T. Wolf, F. Reinhard, L.C.L. Hollenberg, F. Jelezko, J. Wrachtrup, Nat. Phys. 7 (2011) 459.

[13] J.R. Maze, P.L. Stanwix, J.S. Hodges, S. Hong, J.M. Taylor, P. Cappellaro, L. Jiang, M.V.G. Dutt, E. Togan, A.S. Zibrov, A. Yacoby, R.L. Walsworth, M.D. Lukin, Nature 45 (2008) 644.
[14] J.P. Tetienne, T. Hingant, L. Rondin, A. Cavaillès, L. Mayer, G. Dantelle, T. Gacoin, J. Wrachtrup, J.F. Roch, V. Jacques, Phys. Rev. B 87 (2013) 235436.
[15] D.M. Toyli, C.F. de las Casas, D.J. Christle, V.V. Dobrovitski, D.D. Awschalom, Proc. Natl. Acad. Sci. USA 110 (2013) 8417.
[16] F. Grazioso, B.R. Patton, P. Delaney, M.L. Markham, D.J. Twitchen, J.M. Smith, Appl. Phys. Lett. 103 (2013) 101905.
[17] F.Z. Shi, Q. Zhang, P.F. Wang, H.B. Sun, J.R. Wang, X. Rong, M. Chen, C.Y. Ju, F. Reinhard, H.W. Chen, J. Wrachtrup, J.F. Wang, J.F. Du, Science 347 (2015) 1135.
[18] H.B. Liu, M.B. Plenio, J.M. Cai, Phys. Rev. Lett. 118 (2017) 200402.
[19] P.B. Li, Z.L. Xiang, P. Rabl, F. Nori, Phys. Rev. Lett. 117 (2016) 015502.
[20] X.Y. Lu, Z.L. Xiang, W. Cui, J.Q. You, F. Nori, Phys. Rev. A 88 (2013) 012329.
[21] P.B. Li, F. Nori, Phys. Rev. Appl. 10 (2018) 024011.
[22] Z.L. Xiang, S. Ashhab, J.Q. You, F. Nori, Rev. Modern Phys. 85 (2013) 623.
[23] Z.L. Xiang, X.Y. Lu, T.F. Li, J.Q. You, F. Nori, Phys. Rev. B 87 (2013) 144516.
[24] L.T. Hall, P. Kehayias, D.A. Simpson, A. Jarmola, A. Stacey, D. Budker, L.C.L. Hollenberg, Nature Commun. 7 (2016) 10211.
[25] P. Wang, W. Yang, New J. Phys. 17 (2015) 113041.
[26] H.J. Wang, C.S. Shin, S.J. Seltzer, C.E. Avalos, A. Pines, V.S. Bajaj, Nature Commun. 5 (2015) 4135.
[27] A. Ishizaki, G.R. Fleming, Proc. Natl. Acad. Sci. USA 106 (2009) 17255.
[28] Q. Ai, T.C. Yen, B.Y. Jin, Y.-C. Cheng, J. Phys. Chem. Lett. 4 (2013) 2577.
[29] Y.J. Yan, J. Chem. Phys. 140 (2014) 054105.
[30] B.X. Wang, M.J. Tao, Q. Ai, T. Xin, N. Lambert, D. Ruan, Y.C. Cheng, F. Nori, F.G. Deng, G.L. Long, npj Quantum Inf. 4 (2018) 52.
[31] W.M. Witzel, S. Das Sarma, Phys. Rev. B 74 (2006) 035322.
[32] W.M. Witzel, S. Das Sarma, Phys. Rev. Lett. 98 (2007) 077601.
[33] W.M. Witzel, S. Das Sarma, Phys. Rev. B 76 (2007) 241303(R).
[34] W. Yao, R.B. Liu, L.J. Sham, Phys. Rev. B 74 (2006) 195301.
[35] W. Yao, R.B. Liu, L.J. Sham, Phys. Rev. Lett. 98 (2007) 077602.
[36] R.B. Liu, W. Yao, L.J. Sham, New J. Phys. 9 (2007) 226.
[37] S.K. Saikin, W. Yao, L.J. Sham, Phys. Rev. B 75 (2007) 125314.
[38] W. Yang, R.B. Liu, Phys. Rev. B 78 (2008) 085315.
[39] W. Yang, R.B. Liu, Phys. Rev. B 79 (2009) 115320.
[40] L.-S. Li, H.-H. Li, L.-L. Zhou, Z.-S. Yang, Q. Ai, Acta Phys. Sin. 66 (2017) 230601.
[41] L.P. Yang, C. Burk, M. Widmann, S.Y. Lee, J. Wrachtrup, N. Zhao, Phys. Rev. B 90 (2014) 241203(R).
[42] N. Zhao, Z. Wang, R.B. Liu, Phys. Rev. Lett. 106 (2011) 217205.
[43] P. Huang, X. Kong, N. Zhao, F.Z. Shi, P.F. Wang, X. Rong, R.B. Liu, J.F. Du, Nature Commun. 2 (2011) 570.
[44] V. Jacques, P. Neumann, J. Beck, M. Markham, D. Twitchen, J. Meijer, F. Kaiser, G. Balasubramanian, F. Jelezko, J. Wrachtrup, Phys. Rev. Lett. 102 (2009) 057403.
[45] X.K. Song, Q. Ai, J. Qiu, F.-G. Deng, Phys. Rev. A 93 (2016) 052324.
[46] N. Zhao, J.L. Hu, S.W. Ho, J.T.K. Wan, R.B. Liu, Nat. Nanotech. 6 (2011) 242.
[47] Z.Y. Zhou, Y.A. Yan, S. Hughes, J.Q. You, F. Nori, Phys. Rev. A 100 (2019) 042112.
[48] D.A. Redman, S. Brown, R.H. Sands, S.C. Rand, Phys. Rev. Lett. 67 (1991) 3420.
[49] A. Jarmola, V.M. Acosta, K. Jensen, S. Chemerisov, D. Budker, Phys. Rev. Lett. 108 (2012) 197601.
[50] A. Jarmola, A. Berzins, J. Smits, K. Smits, J. Prikulis, F. Gahbauer, R. Ferber, D. Erts, M. Auzinsh, D. Budker, Appl. Phys. Lett. 107 (2015) 242403.
[51] M. Mrózek, D. Rudnicki, P. Kehayias, A. Jarmola, D. Budker, W. Gawlik, EPJ Quantum Technol. 2 (2015) 22.
[52] N. Zhao, S.W. Ho, R.B. Liu, Phys. Rev. B 85 (2012) 115303.
[53] V.V. Dobrovitski, A.E. Feiguin, R. Hanson, D.D. Awschalom, Phys. Rev. Lett. 102 (2009) 237601.
[54] W. Zhang, N. Konstantinidis, K.A.A. Hassanieh, V.V. Dobrovitski, J. Phys. Condens. Matter 19 (2007) 083202.
[55] W.G. Proctor, F.C. Yu, Phys. Rev. 81 (1951) 20.
[56] V. Royden, Phys. Rev. 96 (1954) 543.
[57] S.E. Lillie, D.A. Broadway, J.D.A. Wood, D.A. Simpson, A. Stacey, J.-P. Tetienne, L.C.L. Hollenberg, Phys. Rev. Lett. 118 (2017) 167204.
[58] A. Jarmola, V.M. Acosta, K. Jensen, S. Chemerisov, D. Budker, Phys. Rev. Lett. 92 (2004) 076401.